Experimental study of exclusive ^{2}H$(e,e'p)n$ reaction mechanisms at high Q^2

K.S. Egiyan,[42, 37, *] G. Asryan,[42] N. Gevorgyan,[42] K.A. Griffioen,[41] J.M. Laget,[37, †] S.E. Kuhn,[31] G. Adams,[33]
M.J. Amaryan,[31] P. Ambrozewicz,[13] M. Anghinolfi,[19] G. Audit,[7] H. Avakian,[37] H. Bagdasaryan,[42, 31] N. Baillie,[41]
J.P. Ball,[2] N.A. Baltzell,[36] S. Barrow,[14] V. Batourine,[24] M. Battaglieri,[19] I. Bedlinskiy,[22] M. Bektasoglu,[31, ‡]
M. Bellis,[33, 5] N. Benmouna,[15] B.L. Berman,[15] A.S. Biselli,[12] L. Blaszczyk,[14] S. Bouchigny,[20] S. Boiarinov,[37]
R. Bradford,[5] D. Branford,[10] W.J. Briscoe,[15] W.K. Brooks,[37] S. Bültmann,[31] V.D. Burkert,[37] C. Butuceanu,[41, §]
J.R. Calarco,[28] S.L. Careccia,[31] D.S. Carman,[37] A. Cazes,[36] S. Chen,[14] P.L. Cole,[37, 17] P. Collins,[2] P. Coltharp,[14]
D. Cords,[37, *] P. Corvisiero,[19] D. Crabb,[40] V. Crede,[14] J.P. Cummings,[33] N. Dashyan,[42] R. De Masi,[7] R. De Vita,[19]
E. De Sanctis,[18] P.V. Degtyarenko,[37] H. Denizli,[32] L. Dennis,[14] A. Deur,[37] K.V. Dharmawardane,[31] R. Dickson,[5]
C. Djalali,[36] G.E. Dodge,[31] J. Donnelly,[16] D. Doughty,[8, 37] M. Dugger,[2] S. Dytman,[32] O.P. Dzyubak,[36]
H. Egiyan,[41, 37, ¶] L. El Fassi,[1] L. Elouadrhiri,[37] P. Eugenio,[14] R. Fatemi,[40] G. Fedotov,[27] G. Feldman,[15]
R.J. Feuerbach,[5] R. Fersch,[41] M. Garçon,[7] G. Gavalian,[28, 31] G.P. Gilfoyle,[35] K.L. Giovanetti,[23] F.X. Girod,[7]
J.T. Goetz,[3] A. Gonenc,[13] C.I.O. Gordon,[16] R.W. Gothe,[36] M. Guidal,[20] M. Guillo,[36] N. Guler,[31] L. Guo,[37]
V. Gyurjyan,[37] C. Hadjidakis,[20] K. Hafidi,[1] H. Hakobyan,[42] R.S. Hakobyan,[6] C. Hanretty,[14] J. Hardie,[8, 37]
F.W. Hersman,[28] K. Hicks,[30] I. Hleiqawi,[30] M. Holtrop,[28] C.E. Hyde-Wright,[31] Y. Ilieva,[15] D.G. Ireland,[16]
B.S. Ishkhanov,[27] E.L. Isupov,[27] M.M. Ito,[37] D. Jenkins,[39] H.S. Jo,[20] K. Joo,[37, 9] H.G. Juengst,[31]
N. Kalantarians,[31] J.D. Kellie,[16] M. Khandaker,[29] W. Kim,[24] A. Klein,[31] F.J. Klein,[6] A.V. Klimenko,[31]
M. Kossov,[22] Z. Krahn,[5] L.H. Kramer,[13, 37] V. Kubarovsky,[33] J. Kuhn,[33, 5] S.V. Kuleshov,[22] J. Lachniet,[5, 31]
J. Langheinrich,[36] D. Lawrence,[26] Ji Li,[33] K. Livingston,[16] H.Y. Lu,[36] M. MacCormick,[20] C. Marchand,[7]
N. Markov,[9] P. Mattione,[34] S. McAleer,[14] B. McKinnon,[16] J.W.C. McNabb,[5] B.A. Mecking,[37] S. Mehrabyan,[32]
J.J. Melone,[16] M.D. Mestayer,[37] C.A. Meyer,[5] T. Mibe,[30] K. Mikhailov,[22] R. Minehart,[40] M. Mirazita,[18]
R. Miskimen,[26] V. Mokeev,[27] K. Moriya,[5] S.A. Morrow,[20, 7] M. Moteabbed,[13] J. Mueller,[32] E. Munevar,[15]
G.S. Mutchler,[34] P. Nadel-Turonski,[15] R. Nasseripour,[36] S. Niccolai,[15, 20] G. Niculescu,[30, 23] I. Niculescu,[37, 23]
B.B. Niczyporuk,[37] M.R. Niroula,[31] R.A. Niyazov,[31, 37] M. Nozar,[37] G.V. O'Rielly,[15] M. Osipenko,[19, 27]
A.I. Ostrovidov,[14] K. Park,[24] E. Pasyuk,[2] C. Paterson,[16] S. Anefalos Pereira,[18] J. Pierce,[40] N. Pivnyuk,[22]
D. Pocanic,[40] O. Pogorelko,[22] S. Pozdniakov,[22] B.M. Preedom,[36] J.W. Price,[4] Y. Prok,[40, **] D. Protopopescu,[28, 16]
B.A. Raue,[13, 37] G. Riccardi,[14] G. Ricco,[19] M. Ripani,[19] B.G. Ritchie,[2] F. Ronchetti,[18] G. Rosner,[16] P. Rossi,[18]
F. Sabatié,[7] J. Salamanca,[17] C. Salgado,[29] J.P. Santoro,[6, 37] V. Sapunenko,[37] R.A. Schumacher,[5] V.S. Serov,[22]
Y.G. Sharabian,[37] N.V. Shvedunov,[27] A.V. Skabelin,[25] E.S. Smith,[37] L.C. Smith,[40] D.I. Sober,[6] D. Sokhan,[10]
A. Stavinsky,[22] S.S. Stepanyan,[24] S. Stepanyan,[37] B.E. Stokes,[14] P. Stoler,[33] S. Strauch,[15, 36] M. Taiuti,[19]
D.J. Tedeschi,[36] U. Thoma,[37, 21, 11, ††] A. Tkabladze,[15] S. Tkachenko,[31] L. Todor,[5] C. Tur,[36] M. Ungaro,[33, 9]
M.F. Vineyard,[38, 35] A.V. Vlassov,[22] D.P. Watts,[16, ‡‡] L.B. Weinstein,[31] D.P. Weygand,[37] M. Williams,[5]
E. Wolin,[37] M.H. Wood,[36, §§] A. Yegneswaran,[37] L. Zana,[28] J. Zhang,[31] B. Zhao,[9] and Z.W. Zhao[36]

(The CLAS Collaboration)

[1]*Argonne National Laboratory, Argonne, IL 60439*
[2]*Arizona State University, Tempe, Arizona 85287-1504*
[3]*University of California at Los Angeles, Los Angeles, California 90095-1547*
[4]*California State University, Dominguez Hills, Carson, CA 90747*
[5]*Carnegie Mellon University, Pittsburgh, Pennsylvania 15213*
[6]*Catholic University of America, Washington, D.C. 20064*
[7]*CEA-Saclay, Service de Physique Nucléaire, 91191 Gif-sur-Yvette, France*
[8]*Christopher Newport University, Newport News, Virginia 23606*
[9]*University of Connecticut, Storrs, Connecticut 06269*
[10]*Edinburgh University, Edinburgh EH9 3JZ, United Kingdom*
[11]*Emmy-Noether Foundation, Germany*
[12]*Fairfield University, Fairfield CT 06824*
[13]*Florida International University, Miami, Florida 33199*
[14]*Florida State University, Tallahassee, Florida 32306*
[15]*The George Washington University, Washington, DC 20052*
[16]*University of Glasgow, Glasgow G12 8QQ, United Kingdom*
[17]*Idaho State University, Pocatello, Idaho 83209*
[18]*INFN, Laboratori Nazionali di Frascati, 00044 Frascati, Italy*
[19]*INFN, Sezione di Genova, 16146 Genova, Italy*
[20]*Institut de Physique Nucleaire ORSAY, Orsay, France*

[21]Institute für Strahlen und Kernphysik, Universität Bonn, Germany
[22]Institute of Theoretical and Experimental Physics, Moscow, 117259, Russia
[23]James Madison University, Harrisonburg, Virginia 22807
[24]Kyungpook National University, Daegu 702-701, South Korea
[25]Massachusetts Institute of Technology, Cambridge, Massachusetts 02139-4307
[26]University of Massachusetts, Amherst, Massachusetts 01003
[27]Moscow State University, General Nuclear Physics Institute, 119899 Moscow, Russia
[28]University of New Hampshire, Durham, New Hampshire 03824-3568
[29]Norfolk State University, Norfolk, Virginia 23504
[30]Ohio University, Athens, Ohio 45701
[31]Old Dominion University, Norfolk, Virginia 23529
[32]University of Pittsburgh, Pittsburgh, Pennsylvania 15260
[33]Rensselaer Polytechnic Institute, Troy, New York 12180-3590
[34]Rice University, Houston, Texas 77005-1892
[35]University of Richmond, Richmond, Virginia 23173
[36]University of South Carolina, Columbia, South Carolina 29208
[37]Thomas Jefferson National Accelerator Facility, Newport News, Virginia 23606
[38]Union College, Schenectady, NY 12308
[39]Virginia Polytechnic Institute and State University, Blacksburg, Virginia 24061-0435
[40]University of Virginia, Charlottesville, Virginia 22901
[41]College of William and Mary, Williamsburg, Virginia 23187-8795
[42]Yerevan Physics Institute, 375036 Yerevan, Armenia
(Dated: January 8, 2007)

The reaction ^{2}H$(e, e'p)n$ has been studied with full kinematic coverage for photon virtuality $1.75 < Q^2 < 5.5$ GeV^2. Comparisons of experimental data with theory indicate that for very low values of neutron recoil momentum ($p_n < 100$ MeV/c) the neutron is primarily a spectator and the reaction can be described by the plane-wave impulse approximation. For $100 < p_n < 750$ MeV/c proton-neutron rescattering dominates the cross section, while Δ production followed by the $N\Delta \to NN$ transition is the primary contribution at higher momenta.

For high virtuality of the exchanged photon, the ^{2}H$(e, e'p)n$ reaction is one of the simplest and best ways to investigate high-momentum components of the deuterium wave function, possible modifications to the internal structure of bound nucleons, and the nature of short-range nucleon correlations. To date this reaction was studied only for low Q^2 (< 1 GeV^2) at Saclay, NIKHEF, Mainz and Bates. A survey prior to 1990 can be found in Ref. [1]. In general, the interpretation of these results suffered from large corrections due to final-state interactions (FSIs), meson exchange currents (MECs) and the intermediate Δ contribution.

The Continuous Electron Beam Accelerator Facility (CEBAF) at Jefferson Laboratory (JLab) has opened a new frontier in the study of ^{2}H$(e, e'p)n$ and other $(e, e'p)$ reactions for Q^2 up to 6 GeV^2. The first study of the exclusive ^{2}H$(e, e'p)n$ reaction at JLab has been carried out in Hall A [2]. The cross section was measured as a function of recoil momentum, p_n, up to 550 MeV/c in perpendicular kinematics with $Q^2 = 0.68$ GeV^2. At low (< 300 MeV/c) recoil momentum, these data can be described to within 1-2σ by the Plane Wave Impulse Approximation (PWIA), while at higher momenta FSIs and the Δ contribution must be included. Two new experiments have been carried out at higher Q^2: the first in Hall A [3] for $Q^2 < 3.5$ GeV^2 and the second in Hall B [4]

for $1.75 < Q^2 < 5.5$ GeV^2 which is reported in this letter. We have done a comprehensive study of the ^{2}H$(e, e'p)n$ exclusive reaction with full kinematic coverage, which allows us to identify the dominant mechanisms.

The experiment has been performed using the CEBAF Large-Acceptance Spectrometer (CLAS) [5], which consists of six sectors, each functioning as an independent magnetic spectrometer. Each sector is instrumented with multi-wire drift chambers, time-of-flight scintillator counters covering polar angles $8° < \theta < 143°$, gas-filled threshold Cherenkov counters (CCs) and lead-scintillator sandwich-type electromagnetic calorimeters (ECs) covering $8° < \theta < 45°$. The CLAS was triggered on scattered electrons identified by a coincidence between EC and CC signals in a given sector.

A 5.761 GeV electron beam impinged on a target cell of liquid deuterium about 5 cm long and 0.7 cm in diameter, positioned on the beam axis close to the center of CLAS. The target entrance and exit windows were 15 μm Al foils. A 4 cm vertex cut for the scattered electron selected events from the central part of the target and eliminated events from the windows. The CLAS vertex resolution [5] of $\sigma = 2$ mm allowed us to estimate a background from the windows of $< 0.5\%$ [6].

Electrons and protons from the reaction ^{2}H$(e, e'p)n$ were selected in fiducial regions of CLAS, where the parti-

cle detection efficiency is high and nearly constant. Both the CC and EC were used to distinguish electrons from pions for momenta < 2.8 GeV/c, whereas only the EC was used for momenta > 2.8 GeV/c where the CC became sensitive to pions. Ref. [6] reports that π^- contamination is < 2% depending on Q^2. The data were corrected for this effect. The protons were identified using tracking and time of flight [5].

The electron detection efficiency depends on the drift-chamber inefficiency (2.5%) and the π^- rejection cuts in the EC (2.5%) and the CC (10%), on average. The proton detection efficiency depends on the π^+ rejection cut (2.5%) and the inefficiency of the drift chambers plus the time-of-flight scintillators (10%) [6].

The exclusive $^2\text{H}(e,e'p)n$ events were extracted from the data by requiring the missing mass to be that of the undetected recoil neutron. We measured the differential $^2\text{H}(e,e'p)n$ cross section as a function of Q^2, p_n and θ_n (the neutron polar angle with respect to the momentum transfer direction), integrated it over ϕ_n (the azimuthal angle of the recoil neutron), and corrected it for acceptance and radiative effects. The acceptance corrections were calculated using a Monte Carlo technique for all Q^2, p_n and θ_n bins, and were applied event by event to every bin. The radiative correction factors were calculated using the method described in Ref. [7].

The measured cross sections (points) are shown versus p_n in Figs. 1, 2, and versus θ_n in Figs. 3, 4 for $Q^2 =$ 2, 3, 4 and 5 GeV^2. Statistical errors only are shown. Systematic uncertainties due to the pion contamination, electron and proton detection efficiency, beam intensity measurements, and target density are less than 1%. More important are the uncertainties from the effective target length (3.5%), acceptance corrections (5.5% point to point), background subtractions from the missing mass distributions (2-3% average; 5.5% point to point), and radiative corrections (4%). The total experimental systematic uncertainty is 10% [6].

We have investigated the same reaction theoretically using the most recent predictions of Ref. [8], which have been programmed into a Monte-Carlo code that generates events in the fiducial acceptance of CLAS. We sampled p_n, θ_n, ϕ_n , ϕ_e (the azimuthal angle of the scattered electron) and Q^2 from a flat distribution, and then calculated all remaining momenta and angles constrained by quasi-elastic kinematics. If the electron and the proton fell in the CLAS acceptance we recorded the kinematics of the event in a form of an Ntuple [9] and we weighted it with the corresponding cross section, differential in p_n, θ_n, ϕ_n, Q^2 and ϕ_e. The events were then binned identically to the experimental data using the same cuts. No normalization factors between theoretical and experimental data were used.

This model is an extension of earlier diagrammatic methods [10, 11] to JLab kinematics. It incorporates four amplitudes: the Plane Wave Impulse Approxima-

tion (PWIA), meson exchange currents (MECs), high energy diffractive nucleon-nucleon elastic scattering (FSIs) and intermediate Δ-nucleon rescattering (ΔN). Deuteron wave functions derived from both the Paris [12] and the Argonne V18 [13] potentials were used. The electron couples to the nucleons through a fully relativistic, on-shell nucleon current. The dipole parameterization was chosen for the magnetic form factors of the nucleon. The latest JLab data [14] were used for the proton electric form factor, while the Galster [15] parameterization was selected for the neutron electric form factor. The parameters of the NN amplitude are the same as in Ref. [8], and are fixed by the elastic scattering cross section. The π and ρ exchanges are taken into account in the MEC and ΔN formation amplitudes, as described in Ref. [11]. The electromagnetic $N \to \Delta$ transition form factor $F_{N\Delta}(Q^2) = (1 - Q^2/9)/(1 + Q^2/0.7)^2$ is driven by the world data (MAID parameterization [16]) and specifically by the highest Q^2 measurement [17] in Hall C at JLab. The most recent data set [18] from CLAS is lower by as much as 10% for $Q^2 < 3$ GeV^2 but is similar for $Q^2 > 3$ GeV^2.

The calculated cross sections are shown in Figs. 1, 2, 3, and 4. Systematic uncertainties in the theoretical cross sections come from the on-shell approximation for the electron-nucleon current ($\sim$5%), the parameterization of the NN elastic scattering amplitude ($\sim$10%), and the parameterization of $F_{N\Delta}$ ($\sim$11%). Thus, the systematic uncertainties in the theoretical predictions are $\sim 15\%$ for the full calculations. Since the MEC amplitude in our Q^2 range is very small, the corresponding uncertainty can be neglected.

Figs. 1 and 2 show the distributions in recoil neutron momentum integrated over the angular range $20° < \theta_n < 160°$, where acceptance corrections are well defined [6]. The experimental p_n distribution drops by three orders of magnitude over the range 0–2 GeV/c similar to the full theoretical calculations. For $p_n < 800$ MeV/c, however, the data and calculations agree better than for higher p_n. Below $p_n = 250$ MeV/c, quasi-elastic scattering of electrons on protons (the PWIA channel) exhausts the cross section. Neutron-proton FSI dominates for $250 < p_n < 750$ MeV/c, while intermediate Δ production is prominent for $p_n > 750$ MeV/c, bringing the model close to the data. Both Paris [12] and Argonne V18 [13] wave functions show similar results for $p_n < 1$ GeV/c, whereas above 1 GeV/c the two wave functions differ strongly, and lead to very different PWIA contributions. However, the ΔN channel overwhelms the cross section here: low momentum components of the wave function feed these higher values of p_n, and the sensitivity of the cross section to the high momentum components of the wave function is lost. Nevertheless, the theory agrees well with the data.

Although the theory describes the neutron momentum distributions well, the log scale makes a close comparison difficult. The remaining differences between theory and
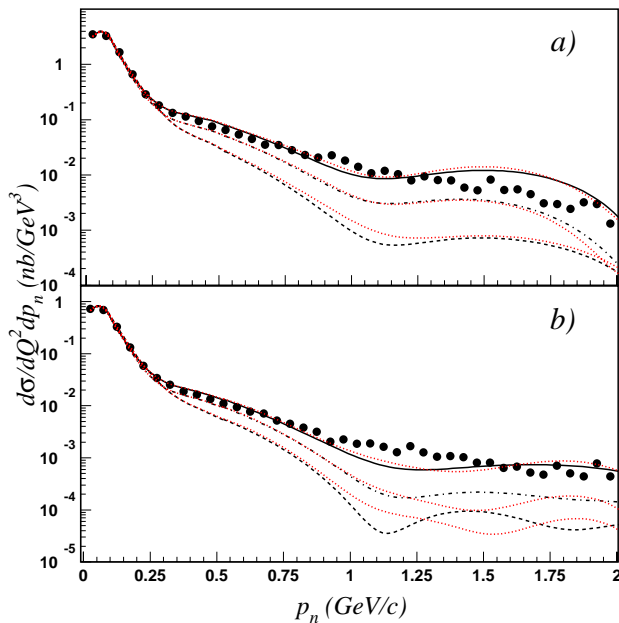
FIG. 1: Color online. The recoil neutron momentum distribution for (a) $Q^2 = 2 \pm 0.25$ GeV^2 and (b) $Q^2 = 3 \pm 0.5$ GeV^2. Dashed, dash-dotted and solid curves are calculations with the Paris potential for PWIA, PWIA+FSI and PWIA+FSI+MEC+NΔ, respectively. Dotted (red) curves are calculations with the AV18 potential.

FIG. 2: Color online. The same as Fig.1 for (a) $Q^2 = 4 \pm 0.5$ GeV^2 and (b) $Q^2 = 5 \pm 0.5$ GeV^2.

experiment are best seen quantitatively in the linear plots of angular distributions for various regions in p_n below 600 MeV/c. The detailed theoretical investigations in Refs. [19, 20] have shown that there are specific features of recoil neutron angular distributions for different ranges in p_n. For $p_n < 0.1$ GeV/c the angular distributions are expected to be insensitive to FSIs, for $p_n \sim 0.4 - 0.5$ GeV/c FSIs should dominate, and for $0.2 < p_n < 0.3$ GeV/c the interference between PWIA and FSI amplitudes should contribute. Until now, this characteristic behavior of the recoil neutron angular distributions has not been checked experimentally.

Figs. 3 and 4 show neutron angular distributions for three ranges of p_n at $Q^2 = 2, 3, 4$ and 5 GeV^2. Each panel clearly shows the evolution of the interaction effects with p_n and θ_n, for a fixed value of Q^2.

In the highest momentum range ($0.4 < p_n < 0.6$ GeV/c) the angular distributions exhibit a large peak in the vicinity of $\theta_n = 70°$. This effect comes from neutron-proton rescattering, and corresponds to the on-shell propagation of the struck nucleon. It is maximal when the kinematics allow for rescattering on a nucleon almost at rest [10], which happens when $x = Q^2/2M\nu = 1$ (ν is the energy of the virtual photon, and M is the nucleon mass). The following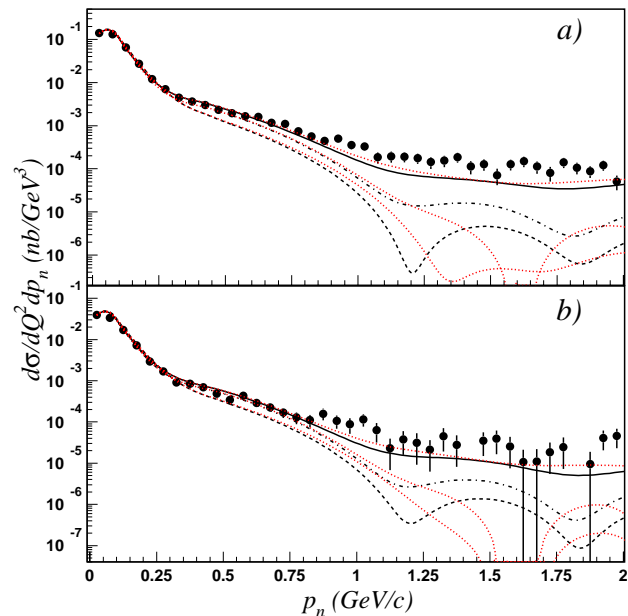 physical picture emerges. The electron scatters primarily from a proton almost at rest. Since the total energy is larger than the sum of the masses of the two nucleons, the struck proton can propagate on-shell and rescatter off the neutron which is also nearly at rest. In the lab frame, the soft neutron recoils at 90° with respect to the fast forward proton. Two-body kinematics places the rescattering peak at about $\theta_n = 70°$ for our kinematics. In the classical Glauber approximation, the nucleon propagator is linearized and recoil effects are neglected, and herefore, the rescattering peak stays at $\theta_n = 90°$ [21, 22]. This has been fixed in the Generalized Eikonal Approximation (GEA) [19] which takes into account higher order recoil terms in the nucleon propagator. In the diagrammatic approach the full kinematics are taken into account from the beginning [8, 10]. The shape of the angular distribution reflects the momentum distribution of the proton in deuterium.

A Δ resonance produced on a nucleon at rest at $x = [1 + (M_\Delta^2 - M^2)/Q^2]^{-1} < 1$, can propagate on-shell and rescatters from the second nucleon also at rest [8]. This contribution shifts the rescattering peak toward larger angles, and brings the theory into better agreement with experiment. It also decreases faster with Q^2, consistent with the steeper variation of the $N \to \Delta$ transition electromagnetic form factor as compared to the dipole parameterization of the nucleon form factors. The excess theoretical cross section at $Q^2 = 2$ GeV^2 is a reflection of our linear fit to the ratio of $N \to \Delta$ and dipole form factors. A better fit to the latest data [18] from CLAS

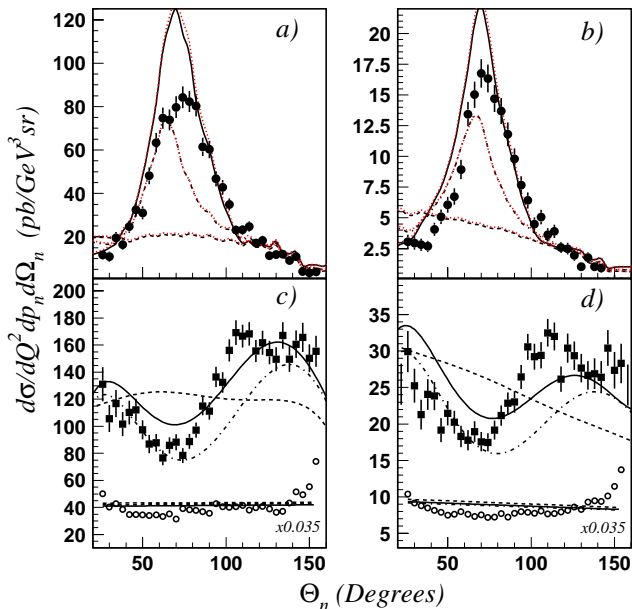FIG. 3: Color online. The recoil neutron angular distribution for (a) $Q^2 = 2 \pm 0.25$ GeV^2, $400 < p_n < 600$ MeV/c; (b) $Q^2 = 3 \pm 0.5$ GeV^2 $400 < p_n < 600$ MeV/c; (c) $Q^2 = 2 \pm 0.25$ GeV^2, $200 < p_n < 300$ MeV/c; and (d) $Q^2 = 3 \pm 0.5$ GeV^2, $200 < p_n < 300$ MeV/c. The data for $p_n < 100$ MeV/c are plotted in the bottom part of (c) and (d) and scaled by 0.035. The curves have the same meaning as in Fig. 1.

FIG. 4: Color online. The same as in Fig 3, but for $Q^2 = 4 \pm 0.5$ GeV^2 ((a) and (c)) and $Q^2 = 5 \pm 0.5$ GeV^2 ((b) and (d)).

leads to a reduction of the peak by ~ 15 % for $Q^2 < 3$ GeV^2, in better agreement with experiment.

In the intermediate momentum range ($0.2 < p_n < 0.3$ GeV/c), FSIs suppress the quasi-elastic contribution in the vicinity of $x = 1$. Here the relative kinetic energy between the outgoing proton and neutron $T \sim Q^2/2M$ lies between 1 and 3 GeV. The nucleon-nucleon scattering amplitude is almost purely absorptive and the FSI amplitude interferes destructively with the quasi-free amplitude. This induces a loss of flux for fast protons.

In the lowest momentum range ($p_n < 0.1$ GeV/c) rescattering effects are small, and the experimental and theoretical angular distributions are similarly flat. The magnitude of the experimental cross sections is well reproduced at low Q^2, but the theory slightly exceeds the data at larger Q^2. This effect has already been observed in the study of ^{3}He$(e, e'p)^2$H at low recoil momentum [23], and is not yet well understood.

In summary, this benchmark experiment demonstrates that the mechanisms of the exclusive ^{2}H$(e, e'p)n$ reaction are well understood for $1.75 < Q^2 < 5.5$ GeV^2. Theoretical and experimental cross sections agree within 20%, 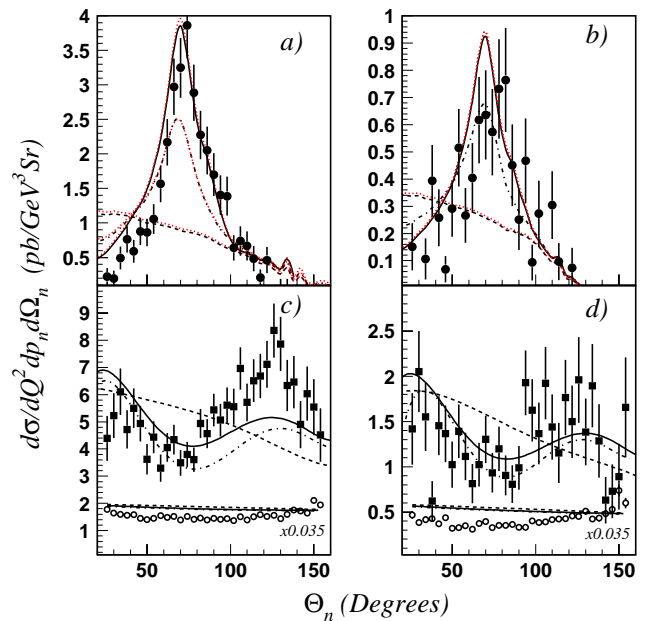consistent with the systematic uncertainties ($\approx 15\%$ for theory and $\approx 10\%$ for experiment). Proton-neutron rescattering (FSIs) and Δ production dominate over a large part of the phase space, except at backward angles ($\theta_n > 110°$) or very low recoil momenta ($p_n < 100$ MeV/c), where the distributions directly reflect the deuteron wave function. A good understanding of the mechanisms of the exclusive ^{2}H$(e, e'p)n$ reaction in our Q^2 region opens an opportunity to investigate the short distance properties of nucleons in deuterium, which will be discussed in our future publications.

* Deceased

† Electronic address: laget@jlab.org; Corresponding author.

‡ Current address: Ohio University, Athens, Ohio 45701

§ Current address: University of Regina, Regina, SK S4S0A2, Canada

¶ Current address: University of New Hampshire, Durham, New Hampshire 03824-3568

** Current address: Massachusetts Institute of Technology, Cambridge, Massachusetts 02139-4307

†† Current address: Physikalisches Institut der Universitaet Giessen, 35392 Giessen, Germany

‡‡ Current address: Edinburgh University, Edinburgh EH9 3JZ, United Kingdom

§§ Current address: University of Massachusetts, Amherst, Massachusetts 01003

[1] J.M. Laget, In: *Modern Topics in Electron Scattering.* Eds. B. Frois and I. Sick. World Scientific 1991, p.290.

[2] P. Ulmer *et al.*, Phys. Rev. Lett. **89**, 062301 (2002).

[3] W. Boeglin *et al.*, JLab Exp E-01-020.

[4] K.Sh. Egiyan, K. Griffioen and M. Strikman, JLab Experiment E-94-019.

[5] B.A. Mecking *et al.*, NIM. A **503**, 513 (2003).

[6] K.Sh. Egiyan, *et al.*, CLAS-Note 2006-025, http://www1.jlab.org/ul/Physics/Hall-B/clas/.

[7] J. Schwinger, Phys. Rev. **76**, 790 (1949).

[8] J.M. Laget, Phys. Lett. **B609**, 49 (2005).

[9] R. Brun *et al.*, HBOOK, CERN Program Library Y250.

[10] J.M. Laget, Phys. Rep. **69**, 1 (1981).

[11] J.M. Laget, Nucl. Phys. **A579**, 333 (1994).

[12] M. Lacombe *et al.*, Phys. Lett. **B101**, 139 (1981).

[13] J. Forest *et al.*, Phys. Rev. C **54**, 646 (1996).

[14] O. Gayou *et al.*, Phys. Rev. Lett. **88**, 092301 (2002).

[15] S. Galster *et al.*, Nucl. Phys. **B32**, 221 (1971).

[16] S.S. Kamalov *et al.*, Phys. Rev. C **64**, 032201 (2002).

[17] V.V. Frolov *et al.*, Phys. Rev. Lett. **82**, 45 (1999).

[18] M. Ungaro *et al.*, Phys. Rev. Lett. **97**, 112003 (2006).

[19] L.L. Frankfurt, M.M. Sargsian and M.I. Strikman, Phys. Rev. C **56**, 1124 (1997).

[20] J.M. Laget, In: *Workshop on Color Transparency (CT97).* Eds. E. Voutier, Grenoble 1997; http://isnpx0162.in2p3.fr/polder/ct97/Jlag/Jlag.html.

[21] A. Bianconi *et al.*, Phys. Rev. C **53**, 576 (1996).

[22] C. Ciofi degli Atti, L.P. Kaptari and D. Treleani, Phys. Rev. C **63**, 044601 (2001).

[23] E. Penel-Nottaris, Ph.D. Thesis, University of Grenoble, July 2004.